

## Rockfall hazard assessment along a road in the Sorrento Peninsula, Campania, southern Italy

B. Palma · M. Parise · P. Reichenbach · F. Guzzetti

Received: 19 February 2010 / Accepted: 4 July 2011  
© Springer Science+Business Media B.V. 2011

**Abstract** Rockfalls are common in the steep and vertical slopes of the Campania carbonate massifs and ridges, and frequently represent the main threat to the anthropogenic environment, potentially damaging urban areas, scattered houses, roads, etc. Despite the generally limited volumes involved, the high velocity of movement (from few to tens of metres per second) poses rockfalls among the most dangerous natural hazards to man. Evaluating the rockfall hazard is not an easy task, due to the high number of involved factors, and particularly to the difficulty in determining the properties of the rock mass. In this paper, we illustrate the assessment of the rockfall hazard along a small area of the Sorrento Peninsula (Campania region, southern Italy). Choice of the site was determined by the presence of a road heavily frequented by vehicles. In the area, we have carried out detailed field surveys and software simulations that allow generating simple rockfall hazard maps. Over twenty measurement stations for geo-mechanical characterization of the rock mass have been distributed along a 400-m-long slope of Mount Vico Alvano. Following the internationally established standards for the acquisition of rock mass parameters, the main kinematics have been recognized, and the discontinuity families leading to the different failures identified. After carrying out field experiments by artificially releasing a number of unstable blocks on the rock cliff, the rockfall trajectories along the slope were modelled using 2-D and 3-D programs for rockfall analysis. The results were exploited to evaluate the rockfall hazard along the threatened element at risk.

---

B. Palma  
Idrogeo s.r.l., Vico Equense, NA, Italy  
e-mail: info@idrogeo.it

M. Parise (✉)  
CNR-IRPI, Bari, Italy  
e-mail: m.parise@ba.ipri.cnr.it

P. Reichenbach · F. Guzzetti  
CNR-IRPI, Perugia, Italy  
e-mail: Paola.Reichenbach@ipr.cnr.it

F. Guzzetti  
e-mail: Fausto.Guzzetti@ipr.cnr.it

**Keywords** Rockfall · Hazard · Modelling · Sorrento Peninsula · Italy

## 1 Introduction

Rockfalls are a type of fast mass movement common in mountain areas worldwide. Rockfalls are triggered by a variety of natural and human-induced causes (Guzzetti and Reichenbach 2010), including earthquakes, freeze–thaw cycles of water, melting of snow or permafrost, temperature changes, intense rainfall, stress relief following deglaciation, volcanic activity, and root penetration and wedging. Human-induced causes of rockfalls include undercutting of rock slopes, mining activities, pipe leakage, inefficient drainage, and vibrations caused by excavations, blasting, or traffic. Individual or multiple rock blocks with volumes ranging from a few cubic decimetres to thousands of cubic metres and travelling at rapid to extremely rapid velocity ( $>3 \text{ m min}^{-1}$ , Cruden and Varnes 1996) make rockfalls dangerous to the population, the built-up environment, and the infrastructure (Whalley 1984; Evans and Hungr 1993; Flageollet and Weber 1996).

In Italy, rockfalls represent a primary cause of landslide fatalities (Guzzetti 2000; Guzzetti et al. 2005). Inspection of the geographical distribution of fatal landslide events in Italy (Salvati et al. 2003, 2010) reveals that in the Campania region the geological and morphological conditions are prone to rockfalls, and the hazard posed by rockfalls is severe (Parise 2002). In particular, the Sorrento Peninsula, along the Tyrrhenian coast between Naples and Salerno, is as a “hot spot” with frequent fatal rockfall events.

In this work, we present the results of an attempt to evaluate rockfall hazard in a section of the Sorrento Peninsula. More specifically, the study is aimed at determining rockfall hazard in an 850-m-long segment of a road built along the steep slopes of Monte Vico Alvano (Fig. 1). Rockfall hazard in the area is determined through numerical simulations of rockfall trajectories. The simulations are performed using four computer codes. Geological and morphological information required to perform the rockfall simulations was obtained from existing topographical and geological maps, and during dedicated field surveys. The results obtained with the different rockfall modelling software are compared and tested against independent information on rockfall occurrence obtained during the field surveys, analysing rockfall trajectories observed in the field when unstable rock blocks were released artificially.

## 2 Regional and local setting

The Sorrento Peninsula is a SW–NE-trending horst that separates the Campania plain, to the north, from the Gulf of Salerno, to the south. It is characterized by a NW-dipping monocline where sedimentary and volcanic rocks, Mesozoic to Recent in age, crop out. Specifically, a sequence of dolomite and limestone is overlaid by Miocene sandstone, preserved chiefly in small structural depressions, by Quaternary alluvial and marine sediments, and by pyroclastic deposits resulting from the explosive activity of the Vesuvius and the Campi Flegrei volcanoes. The structural setting is dominated by NW–SE- and NE–SW-trending normal faults and thrusts, which locally exhibit a strike-slip component (Patacca and Scandone 1987; Cinque et al. 1993). Morphology is characterized by steep to very steep slopes, the result of the complex interaction between uplift, controlled chiefly by block faulting, and erosion.

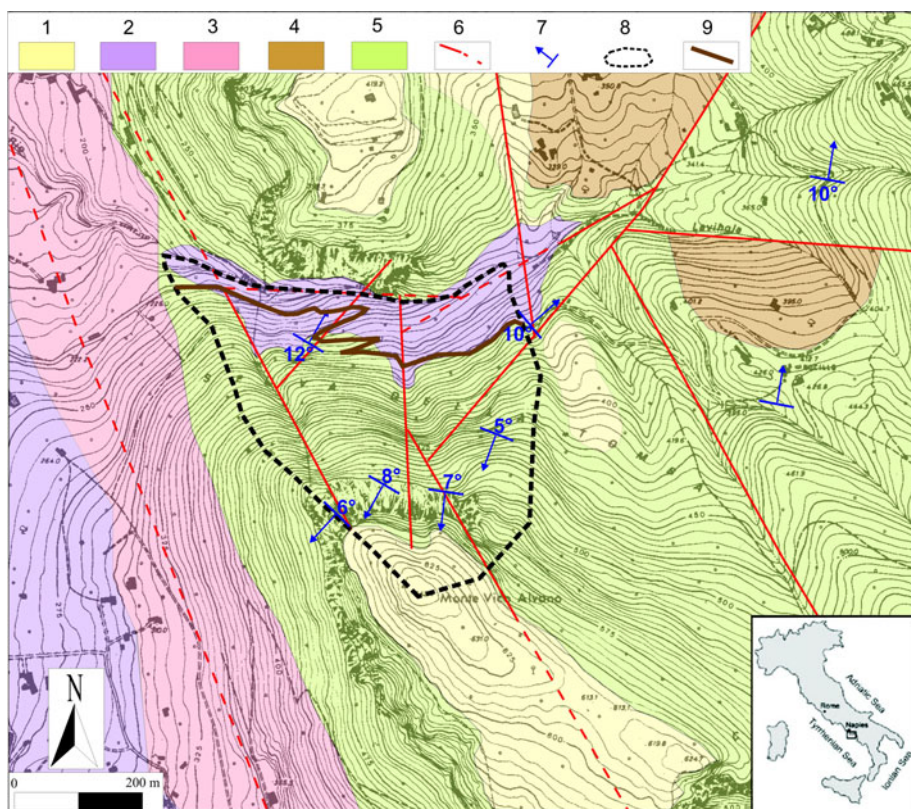


**Fig. 1** Location of the study area and geological map: 1 Fall pyroclastic deposits (Holocene–Upper Pleistocene); 2 Slope debris (Holocene–Pleistocene); 3 Conglomerates (Upper Pleistocene); 4 Sandstones and calcareous marls (Lower Tortonian); 5 Limestones (Upper Cretaceous); 6 Tectonic discontinuities (*dashed when inferred*); 7 Strata bedding; 8 boundary of the investigated slope; 9 Via Lavinola

Mass movements are abundant in the Sorrento Peninsula, where they have resulted in multiple catastrophic events that have caused damage to the population, the infrastructure, and the built-up environment (Budetta and Santo 1994; Calcaterra and Santo 2004). Due to the local morphology, the main transportation network runs primarily along the seashore and at the bottom of high and steep to sub-vertical rock slopes prone to rockfall failures. For this reason, roads in the area are frequently affected by rockfalls. Given the extent of the rockfall problem, protection of the transportation network from rockfalls is problematic in the Sorrento Peninsula (Budetta and Santo 1994).

The study area is located along the southern slopes of Monte Vico Alvano (Fig. 1), consisting of layered limestone, Cretaceous in age, covered by sandstone and calcareous marl, Miocene in age, and by thin and partially reworked pyroclastic deposits, including a pumice layer from the 79 AD eruption of Vesuvius described by Pliny the Younger. The top of the ridge is an old (relict), low gradient surface, separated from the foothills by steep to sub-vertical fault-scarp-slopes affected by multiple slope instabilities, chiefly rockfalls. In the rockfall source area, the size of the individual failures depends on the mechanical properties of the rock, which in places is highly fractured.

### 3 Geo-mechanical analysis

In the study area, a detailed geological and structural survey conducted in the period from 2002 to 2007 allowed determining the geo-mechanical characteristics of the rockfall source areas and obtaining information on rockfall trajectories. Due to the morphology of the area, characterized by very steep and locally inaccessible slopes, the geological and structural survey was difficult to perform. First, the most accessible sites were studied. However, the location and the reduced number of accessible sites were such that the information obtained at these sites was not sufficient for a reliable characterization of the geo-mechanical properties of the rock mass. This is a common problem in mountain areas, where terrain is inaccessible or difficult to reach (Terzaghi 1965; LaPointe and Hudson 1985; Dershowitz and Einstein 1988). To obtain geo-mechanical information for a spatially distributed and sufficiently large number of sites on the rock cliff, alpine techniques were used. Investigators climbed on the rock cliff and performed a systematic survey of the rock face along horizontal and vertical profiles. The information obtained at individual measuring stations positioned along the profiles was integrated with comparable information obtained at known rockfall source areas (Guadagno 2005).

At each of the twenty measuring stations, macro- and meso-scopic structural analyses were performed to obtain quantitative information on the type, number, orientation, spacing, aperture, persistence, and filling of the rock discontinuities (Hoek and Bray 1981; Hudson and Priest 1983) (Table 1; Figs. 2, 3). Geo-mechanical data were collected adopting the standards proposed by the International Society of Rock Mechanics (ISRM 1978). Many fractures were found open, with aperture chiefly lower than 5 mm and rarely larger than 10 mm. Most of the open fractures were empty and did not contain filling material. The individual discontinuities were analysed visually to determine prevailing direction of movements based on local kinematic indicators, including slickensides on fault and joint planes. Given the type of rock cropping out in the area (i.e., layered and fractured limestone), care was taken in the identification and quantification of weathering effects on the individual discontinuities, resulting from a combination of physical alteration and chemical solution (Fookes and Hawkins 1988; Parise 2008).

In addition to measuring the geo-mechanical properties of the individual discontinuities, at each measuring station the shape and size of individual or multiple unstable rock blocks were estimated. The volume of the single blocks was obtained by measuring the distance between adjacent discontinuities and by estimating the pervasiveness and depth of the discontinuities in the rock mass. The most frequent rock blocks were small in size, ranging in volume  $10 < V_L < 50 \text{ cm}^3$ , with only a few blocks with volume  $V_L > 2 \text{ m}^3$  (Table 1). Along the talus slopes below the rock cliff, a number of boulders were identified and measured. The volume of the boulders was  $V_L < 1 \text{ m}^3$ , possibly as a result of fragmentation at rockfall impact points. Some of the large boulders were covered by soil and vegetation. This is an indication that most of the slope failures were old. Nevertheless, in recent years several rockfalls have occurred, which forced the local authorities to close the road.

Data on the attitude of the individual discontinuities collected in the field were plotted on equal-area (Lambert) and on equal-angle (Wulff), lower hemisphere stereographic projections (steronets). The equal-area plots were used for density analysis and for the identification of the attitude of the main sets of discontinuities. The analysis revealed that, in addition to bedding, six sets of discontinuities are present in the study area (Table 1; Fig. 3). At each measuring station, at least three sets of discontinuities—including bedding—were identified. Given the spacing of the discontinuities (Table 1), blocks of

**Table 1** Discontinuities identified during the geological-structural surveys

Station (with discontinuities number)	Slope	Family	Random						Bedding						Romania class	Block size (Palmström 1996)		
			k1			k2			k3			k4			k6			
			Dip	Dip	Dip	Dip	Dip	Dip	Dip	Dip	Dip	Dip	Dip	Dip	Dip	dip	dip	dip
1 (40)	344	85	318	89	203	85	66	89	278	79	278	79	278	79	224	6	II	0.18
2 (69)	25	85	321	88	29	86	175	82	210	8	210	8	210	8	IV	1.22		
3 (16)	312	75	210	76	210	76	175	82	114	5	114	5	114	5	II	0.19		
4 (27)	315	85	326	89	36	78	65	88	189	7	189	7	189	7	I	1.20		
5 (29)	330	80	146	87	39	82	204	80	54	86	204	80	204	80	187	6	III	4.57
6 (44)	70	85	150	87	204	80	67	83	174	75	204	80	204	80	213	6	II	1.20
7 (73)	250	85	220	82	77	81	162	74	115	81	220	82	220	82	202	5	III	3.57
8 (35)	320	85	139	87	40	80	193	62	77	81	193	62	193	62	177	5	III	0.33
9 (31)	60	80	139	87	40	80	220	80	253	62	177	52	177	52	203	6	III	0.23
10 (44)	315	85	140	78	200	66	236	84	194	83	200	66	200	66	32	22	III	0.17
11 (23)	315	90	304	84	77	57	184	71	293	68	304	84	304	84	142	25	III	2.03
12 (21)	358	90	140	75	170	67	177	69	148	44	140	67	140	67	139	5	II	0.49
13 (12)	325	90	324	57	160	70	177	69	142	59	324	57	324	57	127	19	III	0.79
14 (44)	346	90	315	80	222	81	177	69	148	44	346	90	346	90	162	2	II	0.33
15 (23)	72	90	321	69	41	81	170	67	148	44	355	85	148	44	163	10	III	0.19
16 (27)	320	75	41	81	160	70	170	67	142	59	320	75	320	75	112	8	III	1.40
17 (33)	330	85	139	82	30	85	241	83	148	44	330	85	330	85	350	5	II	0.67
18 (36)	320	85	326	80	232	89	160	70	142	59	320	85	320	85	105	4	III	0.11
19 (21)	320	80	144	81	238	83	144	81	148	44	320	80	320	80	129	5	III	0.06
20 (31)	320	80	144	81	238	83	144	81	148	44	320	80	320	80	134	6	III	0.27

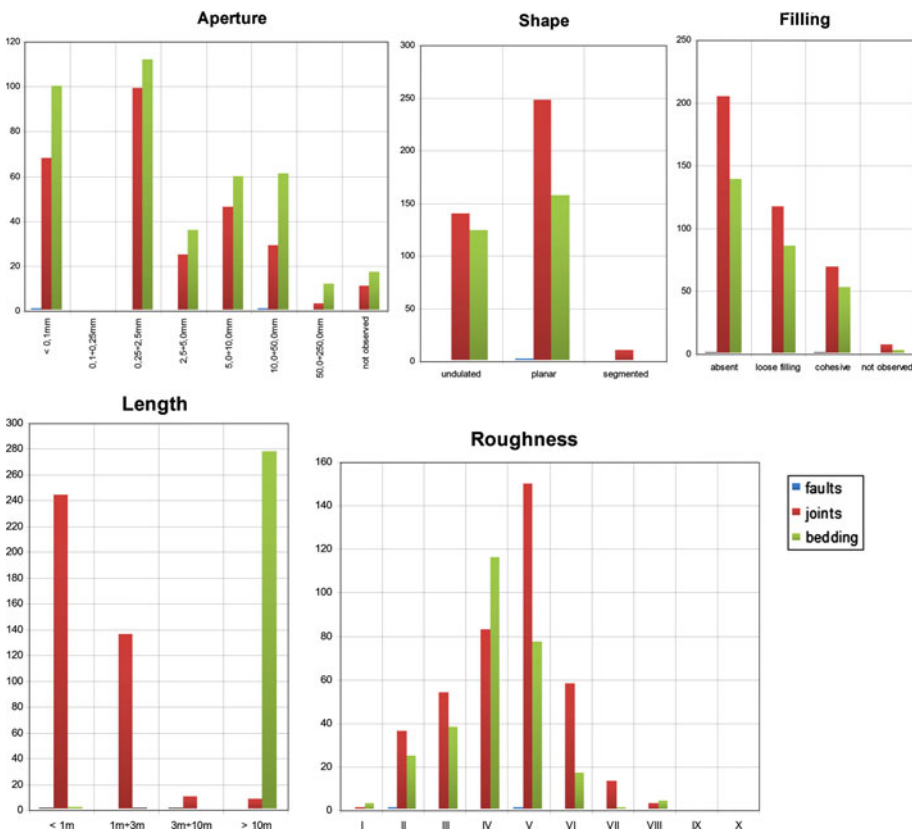


**Fig. 2** Histograms showing the main parameters of surveyed discontinuity systems

generally small to medium size ( $10 < V_L < 50 \text{ cm}^3$ ) are separated from the rock mass. Some of the blocks are balanced precariously (Brune 1996), posing a threat both to the road at the base of the slope and to the traffic along the road.

The equal-angle data were used to perform a set of Markland and Matheson tests (Markland 1972; Matheson 1983). The Markland test compares the orientation of the local slope with the orientation of the discontinuities and the internal angle of friction (the frictional component of the shear strength) of the rock to determine which discontinuity makes the rock mass unstable, theoretically. The Matheson test allows identification of the likely movements in a rock slope by zoning in the stereoplot those sectors more prone to produce different types of instability mechanisms (an example of the test output is presented as Fig. 4). Results of both the tests indicate that most of the potential block failures are of the fall or of the topple types. Topples are associated chiefly with the presence of release joint systems (Fig. 5). Falls are locally associated with the presence of overhanging, unsupported slabs, the result of selective erosion of the clay beds separating limestone beddings. Given the slope aspects in the study area (N 145 and N 235), and the geometrical relationship with the different sets of discontinuities, the most prone sets for detachment of rock blocks are K2 and K3 (Table 1). Potentially unstable conditions are most abundant in the upper part of the rock cliff, where limestone layers are thinner and the effect of the stress release is largest.

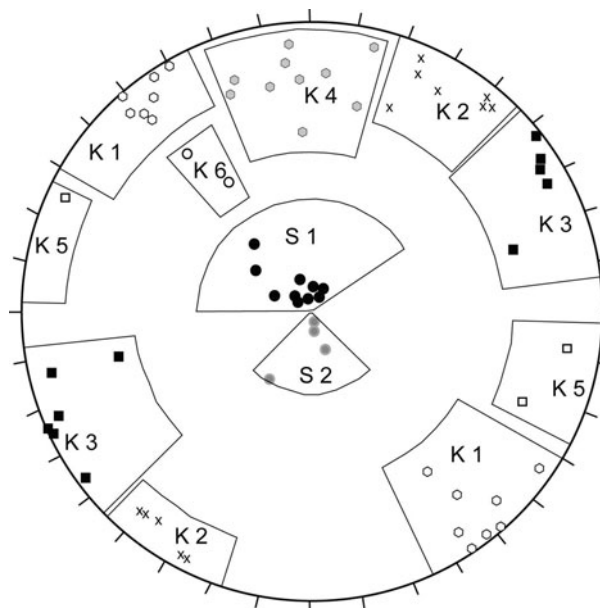


**Fig. 3** Stereoplot showing the six families of tectonic discontinuities (K1 to K6) and the strata bedding (S1 and S2)

The geo-mechanical data obtained at the 20 measurement stations were superimposed on a  $5\text{ m} \times 5\text{ m}$  grid, geographically coherent with a digital elevation model (DEM) available for the study area. The gridded information was used to obtain a spatially distributed evaluation of the stability of the rock cliff, adopting the Slope Mass Rating (SMR) geo-mechanical classification index (Romana 1985, 1991). The SMR index is obtained from the Rock Mass Rating (RMR) system (Bieniawski 1976, 1989), modulated by the addition of four adjustment factors, including three factors to consider the effects of joint and slope orientation ( $F_1$ ,  $F_2$ ,  $F_3$ ) and one factor related to the slope excavation method ( $F_4$ ). For natural slopes,  $F_4 = 15$  (Singh and Goel 1999). The SMR classification index was determined at each measuring station, in five classes (Table 2), and interpolated over the entire rock cliff (Fig. 6). For the interpolation, the lowest (worst) class determined at each measuring station was selected. This is justified because the output of the spatially distributed SMR classification was used to identify the areas more likely to generate rockfalls and as input for the numerical modelling of rockfalls (Dorren 2003; Dorren et al. 2006).

#### 4 Rockfall modelling

To ascertain rockfall hazard in the study area, 2-dimensional (2D) and 3-dimensional (3D) numerical models for rockfall simulation were used, including the following: (1) GeoRock, a 2D model that incorporates the Colorado Rockfall Simulation Program (CRSP) (GeoStru 2004; Pfeiffer and Bowen 1989; Pfeiffer et al. 1991; Jones et al. 2000); (2) Rotomap, which implements a 3D lumped mass model (Scioldo 2006); (3) GeoRock 3D, a total energy

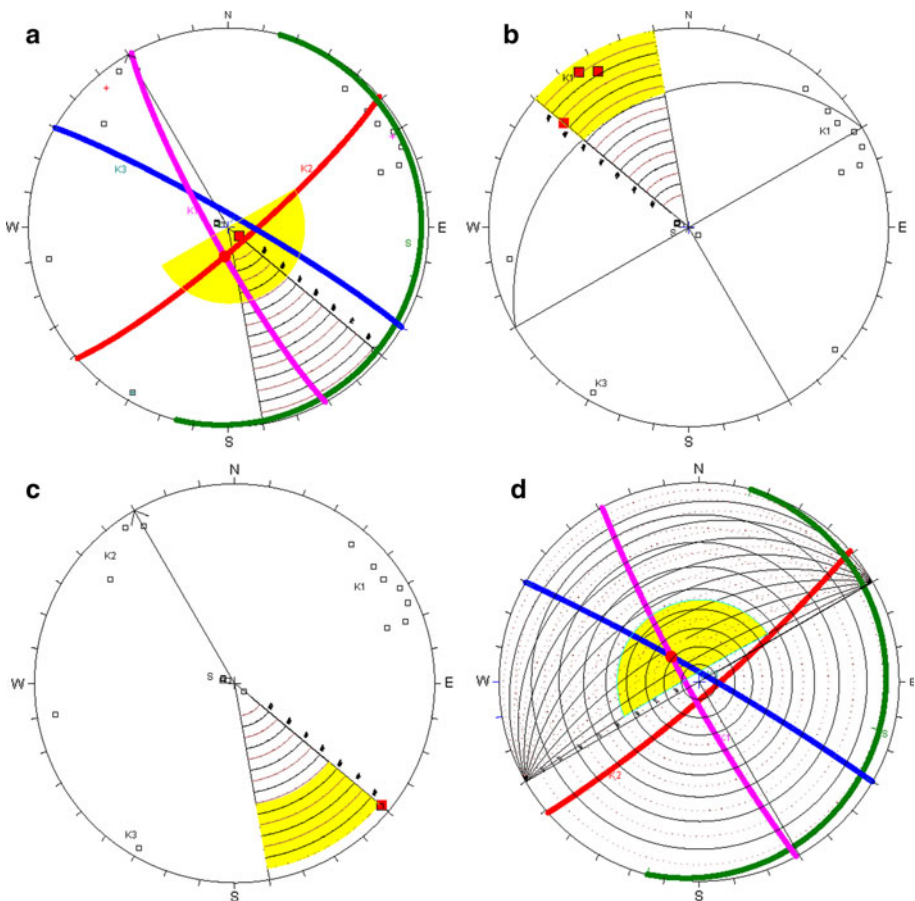


**Fig. 4** Example of the Matheson test performed on one of the measuring station (rock face oriented 330/85). Yellow colour indicates the stereoplot areas prone to possible movements of the following type: **a** toppling failure; **b** flexural toppling; **c** planar sliding; **d** wedge failure. Discontinuity families: K1 in purple, K2 in red, K3 in blue, bedding S in green. Red colour marks the poles and great circles intersections potentially unstable

conservation model (GeoStru 2009); and (4) Stone (Guzzetti et al. 2004), a 3D kinematic (lumped mass) distributed modelling software.

Numerical modelling of rockfall trajectories in the study area was performed in steps. First, the GeoRock 2D software was used to obtain preliminary estimates of the maximum distance to the ground of the rockfall trajectories and of the energy dissipated at impact points. To perform a simulation, the GeoRock 2D software requires the following factors (Table 3): (1) information on the shape, size (volume), weight, and starting velocity of the falling block; (2) values for the normal and the tangential energy restitution coefficients, to model the loss of energy at the impact points; and (3) values for the roughness coefficient, used to model the loss of energy where the block is rolling. Outputs of the modelling software include the following: (1) the type of movement of a block along a falling trajectory, (2) the distance to the ground of the rockfall trajectory, and (3) the energy of the block along the falling trajectory. For this preliminary 2D simulation, eight representative

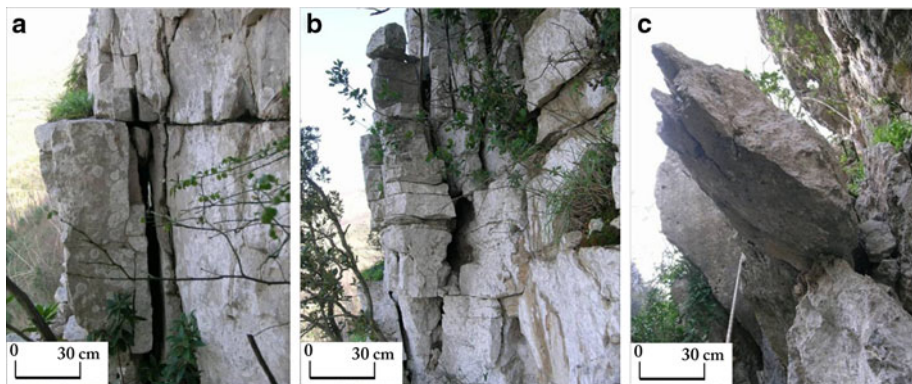


**Fig. 5** Some failure mechanisms identified during the surveys: **a** shear failure controlled by tensional release and bedding planes; **b** complex movement deriving from interaction among the blocks, with planar slide and/or toppling, likely evolving to fall; **c** toppling failure

**Table 2** Romana classification, used for a first zonation of the slope and for the identification of the rockfall source areas

Class	V	IV	III	II	I
SMR	0–20	21–40	41–60	61–80	81–100
Stability	Highly unstable	Unstable	Partially stable	Stable	Completely stable
Failure type	Large planar failures and rotational slumps	Planar failures along several joints and/or large wedges	Planar failures along some joints and/or many wedges	Some failures of isolated blocks	

rockfall source areas were identified along the cliff top, and an ensemble of fourteen topographic profiles was traced from the source areas down the slope along the steepest local terrain gradient.

A first set of 2D rockfall simulation was obtained along the fourteen topographic profiles (Fig. 7), using normal and tangential restitution coefficients obtained from the literature (Hoek 1987; Bieniawski 1989; Pfeiffer and Bowen 1989). Analysis of this first set of simulations revealed that the modelling results were not in agreement with field data, including the location of individual rockfall boulders along the slope. The mismatch was attributed chiefly to incorrect values for the normal and the tangential restitution coefficients adopted for the simulations. To overcome this problem, and to obtain better estimates for the energy restitution and rolling friction coefficients, we performed a set of field experiments. Twenty-four unstable blocks identified on the rock cliff were measured to obtain accurate information on their shape and size, and then artificially released. For each released block, the main impact points and the location of the end point of the rockfall trajectory (the point of deposition) were determined. This empirical information obtained in the field was used to perform a new set of parametric rockfall simulations, using the GeoRock 2D software. A different set of simulation was performed for each of the 24 blocks, releasing from each point 50 boulders that were “launched” using a wide range of energy restitution and rolling friction coefficients from the literature. The ensemble of the

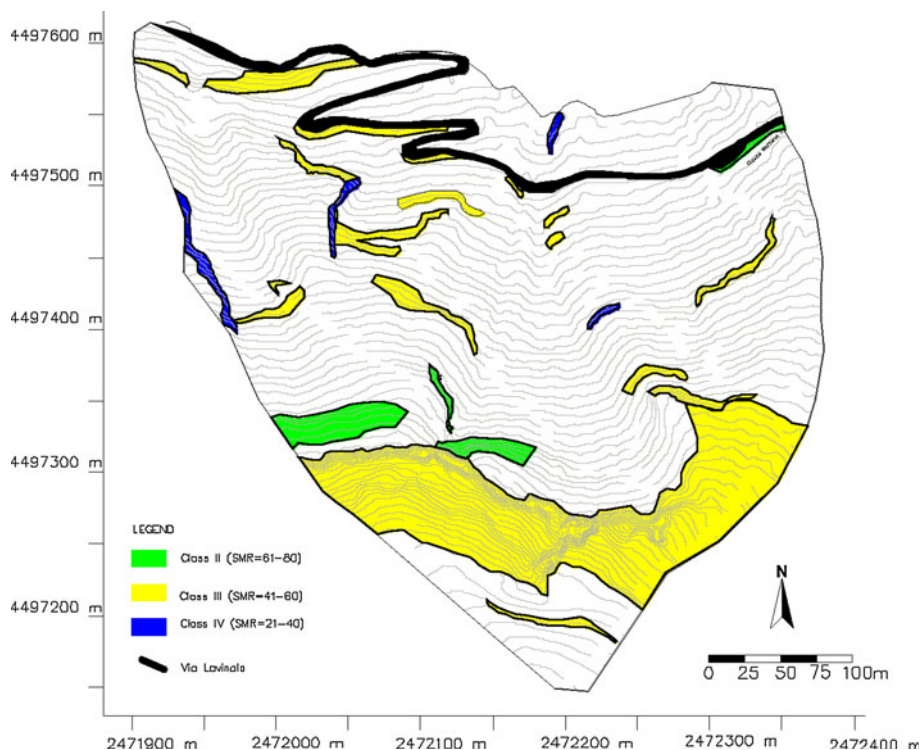


**Fig. 6** Zonation of the study area according to the SMR index. Explanation: green colour is Class II (SMR = 61–80), yellow colour is Class III (SMR = 41–60), and blue colour is Class IV (SMR = 21–40)

obtained rockfall trajectories were compared to the empirical data, and the simulated rockfall trajectories that matched the field data were identified. The energy restitution and rolling friction coefficients used for these modelled rockfall trajectories were taken as representative of the field conditions (see the numbers in Table 3) and used for further 3D modelling of the rockfalls.

For the 3D modelling of the rockfall trajectories, a detailed representation of the topographic surface obtained using a terrestrial laser scanner was used. The digital terrain representation consisted of a digital elevation model (DEM) with a  $5\text{ m} \times 5\text{ m}$  ground resolution. This regularly spaced digital terrain representation was obtained by interpolating irregularly spaced elevation points. Interpolation was performed using kriging.

Rotomap (Scioldo 2006) is a lumped mass model that requires a digital elevation model (DEM), the rockfall source areas, the initial velocity of the block, the limit angle, the maximum angle deviation, and the energy restitution and rolling friction coefficients. The outputs are the geometry of the block trajectories, the arrival points, the maximum energy and the height of the blocks. At Mount Vico Alvano, the trajectories computed by Rotomap (Fig. 8a) confirm those observed during the removal operations of some limestone blocks. Most of the detached blocks, in fact, moved within the slight valley in the central part of the slope and were able to reach the road, posing a serious threat for a long part of the communication route.

**Table 3** Main inputs required by the computer programs

	GeoRock 2D	Rotomap	GeoRock 3D	Stone
Trajectory analysis	2D	3D	3D	3D
Physical model	Total energy conservation	Lumped mass	Lumped mass	Lumped mass
DEM	No	Yes	Yes	Yes
Shape of the block	Spherical	–	–	–
Size of the block	4.6 m <sup>3</sup>	4.6 m <sup>3</sup>	4.6 m <sup>3</sup>	–
Weight of the block	1.2 × 10 <sup>4</sup> kg	1.2 × 10 <sup>4</sup> kg	1.2 × 10 <sup>4</sup> kg	–
Initial velocity of the block	1 m s <sup>-1</sup>	1 m s <sup>-1</sup>	1 m s <sup>-1</sup>	1 m s <sup>-1</sup>
Normal restitution coefficient				
Limestone	0.53	0.53	0.53	0.53
Debris and volcaniclastic cover	0.32	0.32	0.32	0.32
Tangential restitution coefficient				
Limestone	0.9	0.9	0.9	0.9
Debris and volcaniclastic cover	0.8	0.8	0.8	0.8
Source area	Individual	Multiple	Multiple	Multiple (cell)
Number of blocks launched from a source area	50	Variable, depending on the size of the source area	25	20

Using similar input data, we prepared rockfall models with GeoRock 3D and Stone. The GeoRock 3D (GeoStru 2009) requires as input a digital elevation model, the normal and tangential energy restitution coefficients, the source area (including the number of blocks to be launched), the initial velocity of the block, the density and diameter of the block. The outputs are the trajectory (Fig. 8b), velocity, height and kinetic energy of the blocks in movement.

Following the simulations performed with GeoRock (2D), with Rotomap and GeoRock 3D, two defensive barriers were planned and put in place (location shown in Fig. 9), to protect the sections of the road that were most likely to be hit by the moving rockfalls. The trajectories derived from the 3D simulations (Rotomap and GeoRock 3D) were used to establish the location of the retaining structures, whilst height and energy values of the barriers were determined using the output obtained by the 2D analysis.

The residual hazard along the road was eventually assessed taking into account the presence of these rockfall defence measures (the rockfall retaining structures). For the purpose, we used Stone (Guzzetti et al. 2002, 2004), a physically based software capable of modelling rockfall processes in three dimensions and of providing information relevant to ascertain rockfall hazard. The software adopts a “lumped-mass” approach to model rockfalls. The falling boulder is considered dimensionless (i.e., a point), and a kinematical simulation is performed. The input data we used for the simulation include (1) the location of the eight rockfall detachment areas, (2) a digital elevation model, and (3) the coefficients of dynamic rolling friction and of normal and tangential energy restitution. Figure 8 shows the cumulative count of rockfall trajectories that passed through each cell and allows evaluating the residual rockfall hazard along the road posed by the areas identified along the cliff top as more representative rockfall source areas.

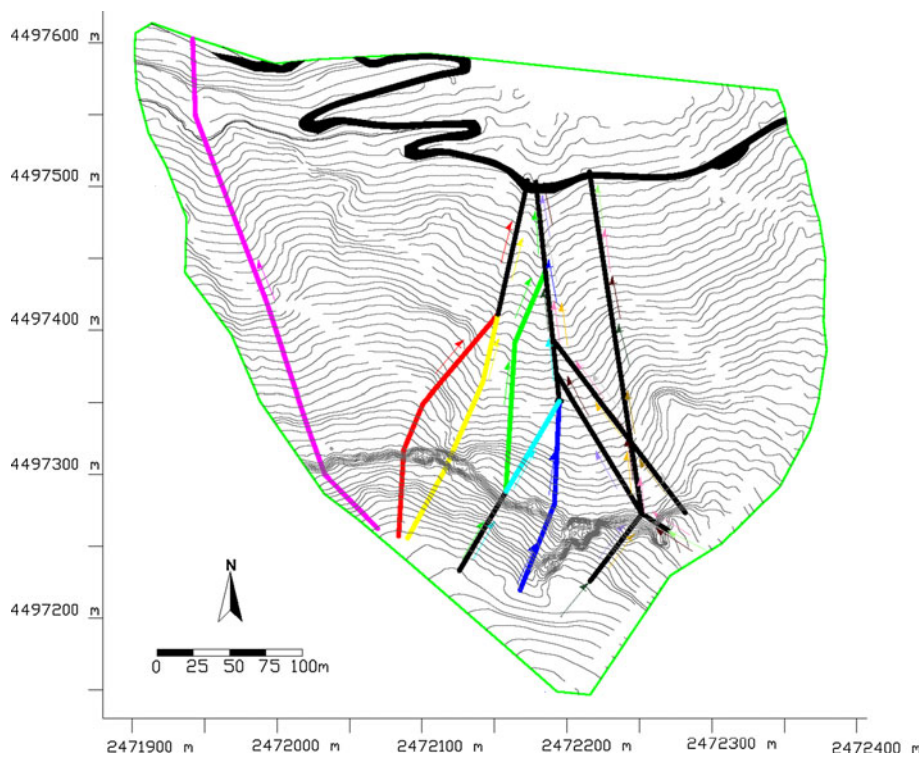


**Fig. 7** Main source areas identified along the slope, and related traces downslope following the highest gradients and the topographic constraints

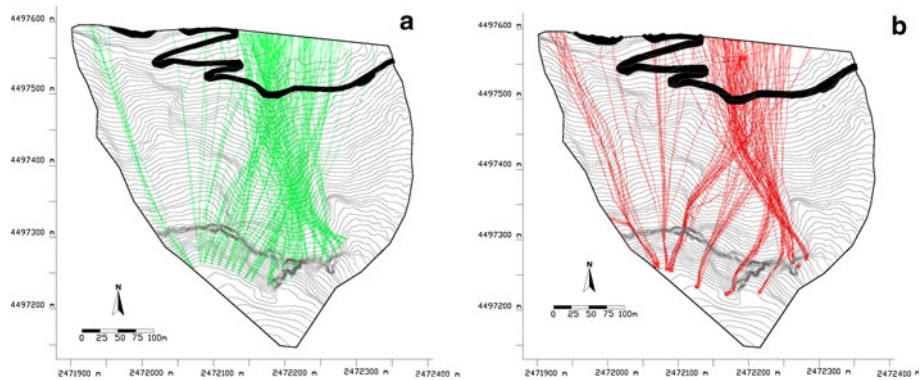


**Fig. 8** Trajectories computed for eight source areas using **a** Rotomap, and **b** GeoRock 3D

## 5 Conclusions

We determined rockfall hazard along the slopes of Monte Vico Alvano through a combination of geological and structural surveys, and 2- and 3-dimensional rockfall numerical modelling (Table 2). The study pointed out to the role played by field surveys, in particular

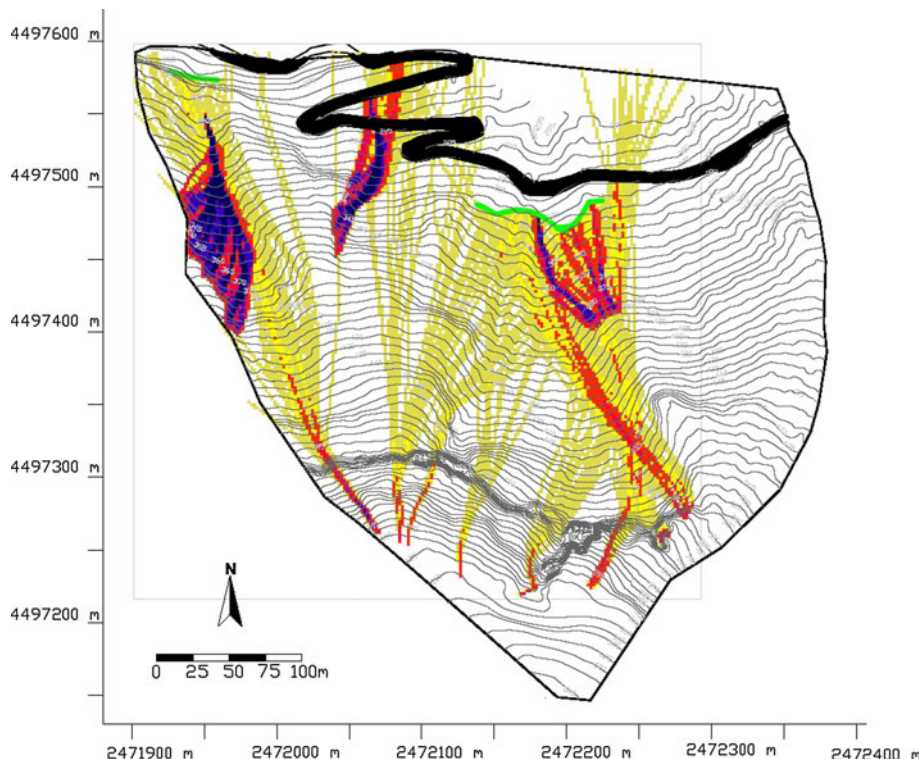


**Fig. 9** Cumulative count of rockfall trajectories using Stone. The simulation consider the presence of rockfall retaining structures (green lines)

those carried out by means of alpine techniques along the vertical cliffs, fundamental for the correct characterization of the rock mass and the identification of the rockfall source areas. Field surveys restricted to the more accessible sites can in fact negatively affect the results of structural surveys, since the collected data represent only partially the real pattern and distribution of the discontinuities in the rock mass.

The second point to highlight regards the reliability of the restitution coefficients available in the literature. Using coefficients acquired from the literature, we obtained not realistic simulations. It appeared therefore of crucial importance the direct observation of falling blocks during the experimental field tests. Field observation allowed us to compute different restitution coefficients that were exploited to perform rockfall back-analysis. The so determined output energy values were eventually used to design the retaining structures. In conclusion, the 2D models were used to calculate the energy values useful to design the defence structures, whilst the 3D models were used to choose the location for the protective measures, based upon the simulated trajectories followed by the blocks. The correct position of the retaining structures and the residual hazard along the road was also evaluated with Stone. Assuming that the retaining structures are effective, the model prepared with Stone reveals that the residual rockfall hazard along the road can be acceptable from the areas classified as more unstable but should be better evaluated considering all the unstable portion of the cliff.

## References

- Bienawski ZT (1976) Rock mass classification in rock engineering. In: Bienawski ZT (ed) Proceedings of the symposium “Exploration for rock engineering”, vol 1, pp 97–106
- Bienawski ZT (1989) Engineering rock mass classifications. Wiley, New York
- Brune JN (1996) Precariously balanced rocks and ground-motion maps for southern California. Bull Seism Soc Am 86:43–54
- Budetta P, Santo A (1994) Morphostructural evolution and related kinematics of rockfalls in Campania (Southern Italy): a case study. Eng Geol 36(3/4):197–210
- Calcaterra D, Santo A (2004) The January 10, 1997, Pozzano landslide, Sorrento Peninsula, Italy. Eng Geol 75(2):181–200
- Cinque A, Patacca E, Scandone P, Tozzi M (1993) Quaternary kinematic evolution of the Southern Apennines. Relationship between surface geological features and deep lithospheric structures. Annali Geofisica 46:249–260
- Cruden DM, Varnes DJ (1996) Landslide types and processes. In: Turner AK, Schuster RL (eds) Landslides. Investigation and monitoring: Transportation Research Board, sp rep 247, pp 36–75
- Dershowitz WS, Einstein HH (1988) Characterizing rock joint geometry with joint system models. Rock Mech Rock Eng 21(1):21–51
- Dorren LKA (2003) A review of rockfall mechanics and modelling approaches. Prog Phys Geogr 27(1):69–87
- Dorren LKA, Berger F, Putters US (2006) Real size experiments and 3D simulation of rockfall on forested and non-forested slopes. Nat Hazards Earth Syst Sci 6:145–153
- Evans SG, Hungr O (1993) The assessment of rockfall hazard at the base of talus slopes. Can Geotechn J 30:620–636
- Flageollet JC, Weber D (1996) Fall. In: Dikau R, Brunsden D, Schrott L, Ibsen ML (eds) Landslide recognition. Wiley, Chichester, England, pp 13–28
- Fooke PG, Hawkins AB (1988) Limestone weathering: its engineering significance and a proposed classification scheme. Quart J Eng Geol 21:7–31
- Geostru (2004) GeoRock user guide. Geostru software, Cosenza, Italy
- Geostru (2009) GeoRock 3D user guide. Geostru software, Cosenza, Italy
- Guadagno G (2005) Rock fall susceptibility at Mount Vico Alvano (Piano di Sorrento). Degree thesis, Univ. Naples “Federico II” (in Italian)
- Guzzetti F (2000) Landslide fatalities and the evaluation of landslide risk in Italy. Eng Geol 58:89–107
- Guzzetti F, Reichenbach P (2010) Rockfalls and their hazard. In: Stoffel M, Boellschweiler M, Butler DR, Luckman BH (eds) Tree rings and natural hazards: a state-of-the-art. Advances in global change research 41. Springer, Heidelberg, pp 129–137. doi:[10.1007/978-90-481-8736-2](https://doi.org/10.1007/978-90-481-8736-2)
- Guzzetti F, Crosta G, Detti R, Agliardi F (2002) STONE: a computer program for the threedimensional simulation of rock-falls. Comput Geosci 28:1079–1093
- Guzzetti F, Reichenbach P, Ghigi S (2004) Rockfall hazard and risk assessment in the Nera River Valley, Umbria Region, central Italy. Environ Manage 34:191–208
- Guzzetti F, Stark CP, Salvati P (2005) Evaluation of flood and landslide risk to the population of Italy. Environ Manage 36:15–36
- Hoek E (1987) RockFall—a program for the analysis of rockfall from slopes. Dept. Civil Engineering, Univ. Toronto, Ontario
- Hoek E, Bray J (1981) Rock slope engineering. Inst Mining Metallurgy, London
- Hudson JA, Priest SD (1983) Discontinuity frequency in rock masses. Int J Rock Mech Min Sci 20(2):73–90
- ISRM (1978) Suggested methods for the quantitative description of discontinuities in rock masses. Int J Rock Mech Min Sci Geomech Abstr 15:319–368
- Jones CL, Higgins JD, Andrew RD (2000) Colorado rockfall simulation program version 4.0. Colorado Department of Transportation, Colorado Geol Survey, Colorado
- LaPointe PR, Hudson JA (1985) Characterization and interpretation of rock mass joint patterns. Geol Soc Am Spec paper 199
- Markland JT (1972) A useful technique for estimating the stability of rock slopes when the rigid wedge sliding type of failure is expected. Imp Coll Rock Mech Res Rep 19:1–10
- Matheson GD (1983) The collection and use of field discontinuity data in rock slope design. Q J Eng Geol 22:19–30
- Parise M (2002) Landslide hazard zonation of slopes susceptible to rock falls and topples. Nat Hazards Earth Syst Sci 2:37–49
- Palmström A (1996) The rock mass index (RMI) applied in rock mechanics and rock engineering. J Rock Mech Tunnel Techn 11(2):1–40

- Parise M (2008) Rock failures in karst. In: Cheng Z, Zhang J, Li Z, Wu F, Ho K (eds), Landslides and engineered slopes. Proceedings of 10th international symposium on landslides, Xi'an, China, 30 June–4 July, 2008, vol 1, pp 275–280
- Patacca E, Scandone P (1987) Post-Tortonian mountain buildings in the Apennines. The role of the passive sinking of a relic lithospheric slab. In: Boriani A (ed) The lithosphere in Italy. Accademia Nazionale dei Lincei, Rome, pp 157–166
- Pfeiffer TJ, Bowen T (1989) Computer simulation of rockfalls. Bull Ass Eng Geol 26(1):135–146
- Pfeiffer TJ, Higgins JD, Schultz R, Andrew RD (1991) Colorado rockfall simulation program. User's manual for version 2.1. Colorado Department of Transportation, Colorado Geological Survey, Colorado
- Romana M (1985) New adjustment ratings for application of Bieniawski classification to slopes. In: International symposium on the role of rock mechanics, Zacatecas, pp 49–53
- Romana M (1991) SMR classification. In: Proceedings of 7th congress on rock mechanics, Aachen, Germany, pp 955–960
- Salvati P, Guzzetti F, Reichenbach P, Cardinali M, Stark CP (2003) Map of landslides and floods with human consequences in Italy. CNR GNDI publ 2822, scale 1:1,200,000
- Salvati P, Bianchi C, Rossi M, Guzzetti F (2010) Societal landslide and flood risk in Italy. Nat Hazards Earth Syst Sci 10:465–483
- Scioldo G (2006) User guide ISOMAP & ROTOMAP—3D surface modelling and rockfall analysis. Geo&Soft International, Torino
- Singh B, Goel RK (1999) Rock mass classification. A practical approach in civil engineering. Elsevier, Amsterdam. ISBN 978-0-08-043013-3
- Terzaghi RD (1965) Sources of error in joint surveys. Geotechnique 15:287–304
- Whalley WB (1984) Rockfalls. In: Brunsden D, Prior DB (eds) Slope stability. Wiley, New York, pp 217–256